A method for estimating tree ring density by coupling CT scanning and ring width measurements: application to the analysis of the ring width–ring density relationship in Picea abies trees

Tojo Ravoajanahary, Frédéric Mothe, Fleur Longuetaud

Estimation of tree ring density by coupling CT scanning and ring width measurements: Application to the analysis of the ring width – ring density relationship in *Picea abies* trees

Tojo Ravoajanahary[a], Frédéric Mothe[a], Fleur Longuetaud[a,*]

[a] *Université de Lorraine, AgroParisTech, INRAE, Silva, 54000 Nancy, France*

Abstract

Tree growth in volume and wood density are the two factors that determine tree biomass. They are important for assessing wood quality and resource availability. Analysing and modelling the relationships between these two factors are important for improving silvicultural practices of softwoods like Norway spruce, for which a negative relationship is generally observed between ring width and ring density.

We describe an original method for obtaining ring density data (RD) by coupling conventional ring width measurements (RW) and air-dry density measurements obtained with X-ray computer tomography at high-speed but with lower resolution than the RW data. The method was applied to 200 discs of Norway spruce trees sampled in a plantation to assess its relevance.

The RW–RD relationship was analysed as a function of cambial age and

*Corresponding author

Email addresses: tojo.ravoajanahary@inrae.fr (Tojo Ravoajanahary), frederic.mothe@inrae.fr (Frédéric Mothe), fleur.longuetaud@inrae.fr (Fleur Longuetaud)

disc height in the stem. Descriptive statistical models were developed and compared to models in the literature. These models made it possible to analyse the variations of RD as a function of height in the tree at a given cambial age or for a given calendar year and also to observe a shift in the juvenile wood – mature wood boundary between the bottom of the tree and the rest of the stem. The RD – RW relationship was observed in the juvenile wood at the base of the stem but not in the juvenile wood higher up. Furthermore, the juvenile wood formed at the base of the tree was denser than the juvenile wood formed higher up and the mature wood formed at the same height.

In conclusion, the proposed method was found to be relevant, especially when wood discs are readily available, and the results obtained highlighted the importance of distinguishing juvenile wood formed at the base of the tree from that formed higher up.

Keywords: Wood density, Ring width, Cambial age, Height in the stem, Juvenile wood, Norway Spruce

---

Title Page

1. **Title of the article:**

   A method for estimating tree ring density by coupling CT scanning and ring width measurements: Application to the analysis of the ring width – ring density relationship in *Picea abies* trees

2. **Author names:**

   - Tojo RAVOAJANAHARY
     Université de Lorraine, AgroParisTech, INRAE, Silva, 54000 Nancy, France
     tojo.ravoajanahary@inrae.fr
   - Frédéric MOTHE
     Université de Lorraine, AgroParisTech, INRAE, Silva, 54000 Nancy, France
     frederic.mothe@inrae.fr
   - Fleur LONGUETAUD*
     Université de Lorraine, AgroParisTech, INRAE, Silva, 54000 Nancy, France
     fleur.longuetaud@inrae.fr

3. **Abstract:**

   Tree growth in volume and wood density are the two factors that determine tree biomass. They are important for assessing wood quality and resource availability. Analysing and modelling the relationships between these two factors are important for improving silvicultural practices of softwoods like Norway spruce, for which a negative relationship is generally observed between ring width and ring density.

   We describe an original method for obtaining ring density data (RD) by coupling conventional ring width measurements (RW) and air-dry density measurements obtained with X-ray computer tomography at high-speed but with lower resolution than the RW data. The method was applied to 200 discs of Norway spruce trees sampled in a plantation to assess its relevance.

   The RW–RD relationship was analysed as a function of cambial age and disc height in the stem. Descriptive statistical models were developed and compared to models in the literature. These models made it possible to analyse the variations of RD as a function of height in the tree at a given cambial age or for a given calendar year and also

to observe a shift in the juvenile wood – mature wood boundary between the bottom of the tree and the rest of the stem. The *RD* – *RW* relationship was observed in the juvenile wood at the base of the stem but not in the juvenile wood higher up. Furthermore, the juvenile wood formed at the base of the tree was denser than the juvenile wood formed higher up and the mature wood formed at the same height.

In conclusion, the proposed method was found to be relevant, especially when wood discs are readily available, and the results obtained highlighted the importance of distinguishing juvenile wood formed at the base of the tree from that formed higher up.

4. **Keywords:**

Wood density; Ring width; Cambial age; Height in the stem; Juvenile wood; Norway Spruce

5. **Acknowledgements:**

Thanks to the forestry cooperative *Forêt et Bois de l'Est* for supplying and delivering the 100 spruce logs to Freiburg. Thanks also to Franka Brüchert of the *Forest Research Institute of Baden-Württemberg* (FVA) and the whole team for their help in organising the measurement and imaging of the logs at FVA. Thanks to Frédéric Bordat, Adrien Contini and Florian Vast for sampling the discs in the field and preparing the samples at INRAE Nancy. Thanks to Adeline Motz and Daniel Rittié for ring width measurements. The authors would like to thank SILVATECH (Silvatech, INRAE, 2018. Structural and functional analysis of tree and wood Facility, doi: 10.15454/1.5572400113627854E12) from UMR 1434 SILVA, 1136 IAM, 1138 BEF and 4370 EA LERMAB from the research center INRAE Grand-Est Nancy, and especially Charline Freyburger for the realisation of the X-ray scans.

6. **Declaration:**

- **Funding:**

SILVA laboratory is supported by a grant overseen by the French National Research Agency (ANR) as part of the "Investissements d'Avenir" program (ANR-11-LABX-0002-01, Lab of Excellence ARBRE). SILVATECH facility is supported by the French National Research Agency through the Laboratory of Excellence ARBRE (ANR-11-LABX-0002-01). This research was made possible thanks to the financial support of the *French National Research*

Agency (ANR) in the framework of the *TreeTrace* project, ANR-17-CE10-0016.

- **Conflicts of interest/Competing interests:** The authors declare that they have no conflict of interest.
- **Availability of data and material:** Two datapapers have been written to describe the database generated in the framework of the ANR Treetrace project. All the data used in this article come from the **TreeTrace_spruce** database and will be made available to the research community before the end of 2022 on the Data INRAE repository at: `https://doi.org/10.57745/WKLTJI`
- **Code availability:** Code is available on request.
- **Authors' contributions:**
  - Tojo RAVOAJANAHARY participated to the data collection, performed the data analysis and contributed to the writing.
  - Frédéric MOTHE participated to the funding acquisition, designed the experiment, participated to the data collection, supervised the work, performed the data analysis and contributed to the writing.
  - Fleur LONGUETAUD participated to the funding acquisition and is the coordinator of the ANR Treetrace project, designed the experiment, participated to the data collection, supervised the work, performed the data analysis and contributed to the writing.
- **Ethics approval (include appropriate approvals or waivers)** Not applicable.
- **Consent to participate (include appropriate statements)** All authors agreed with the content.
- **Consent for publication (include appropriate statements)** All authors gave explicit consent for publication.

7. **Key Message**

   The original method proposed provides useful data for the analysis of ring density variations in stems, highlighting the particular behaviour observed at the base of the tree.

1. Introduction

The relationship between ring width (RW) and ring density (RD) has been studied quite extensively for several reasons. RW is included in wood grading standards because it is related to wood density, the latter being an indicator of the mechanical properties and performance of the wood material (Saranpää, 2003; Lin et al., 2007; Kiaei et al., 2012). The properties of fuelwood (Sotelo Montes et al., 2017) and paper (García-Gonzalo et al., 2016) are also related to wood density. The RW–RD relationship has been observed and modelled in many dendrochronological studies that attempt to relate within-ring characteristics to climate variables (e.g., Wimmer and Grabner, 2000; Franceschini et al., 2013) in order to reconstruct past climate or predict tree growth in future climate.

For softwoods, a negative relationship between RW and RD is generally accepted. More specifically, this relationship is mostly observed for species with a gradual transition between early wood and late wood (Todaro and Macchioni, 2011), such as Norway spruce (*Picea abies*). When this negative relationship is observed, it is largely due to the fact that for wide rings, the amount of early wood (of lower density) becomes more important while the amount of late wood (of higher density) remains roughly constant. This negative relationship probably reflects a trade-off between volume growth and density of wood formed, and can be illustrated by a few examples among others. In the context of forest productivity or carbon fluxes, Bouriaud et al. (2015) has worked on this relationship for Norway spruce to improve estimates of annual biomass increments. Indeed, inter-annual density variations must be taken into account to avoid underestimating biomass increments

in years when volume growth is reduced. Over the last century, increased growth associated with decreased wood density has been observed for several species including Norway spruce (Badeau et al., 1996; Franceschini et al., 2010; Bontemps et al., 2013; Pretzsch et al., 2018).

The *RW–RD* relationship has been extensively studied for Norway spruce (e.g., Olesen, 1977; Lindström, 1996b; Wimmer and Downes, 2003; Jyske et al., 2008). The classical profile of radial density variation is described by Olesen (1977) as follows: a decrease from the pith to ring 8-10, followed by an increase and stabilization between the 15^{th} and 20^{th} annual ring, which would correspond to the boundary between juvenile wood (area of high variation in properties) and mature wood. In addition, a density peak near the pith was reported to occur in the second or third ring (Olesen, 1977; Saranpää, 1994). For softwoods, it is accepted that juvenile wood is on average less dense than mature wood (Olesen, 1977; Lachenbruch et al., 2011).

Most of the time for practical reasons the *RW–RD* relationship is studied at 1.30 m, but some studies have focused on its variation with height in the tree, for a given cambial age or for a given calendar year (Olesen, 1977; Saranpää, 1994; Jyske et al., 2008).

The data used to study *RD* profiles and the *RW–RD* relationship are usually obtained by microdensitometry (Jacquin et al., 2017) on wood samples dried at 12%, with equipment such as the SilviScan (e.g., Piispanen et al., 2014) or other X-ray equipments (Jyske et al., 2008; Bouriaud et al., 2015). Conventional microdensitometry provides *RW* and *RD* with high accuracy but requires a significant amount of time to prepare samples of strictly constant thickness (usually 1-2 mm thick) which limits its use. Several meth-

ods have been developed recently to analyse unprepared wood core samples for ring width and density at high resolution (De Mil et al., 2016; Van den Bulcke et al., 2019); but the acquisition of such images is still slow. Faster methods of measuring density from unprepared cores have been developed (Steffenrem et al., 2014; Jacquin et al., 2019; Kerfriden et al., 2021) but the accuracy is lower than conventional microdensitometry and these methods are still limited for the analysis of individual growth rings. On the other hand, the acquisition of wood cores is fast and non-destructive but cores have the disadvantage that they do not always include the first rings close to the pith and represent only a single radius which may not be representative of the entire section (e.g., in the presence of compression wood).

The first objective of this work was to propose a new and complementary method for assigning an average density value to each ring of a disc. The first originality lies in the analysis of the density of a ring on a whole disc rather than a limited number of radii (only one generally in the case of a core), which can lead to biased density measurements in the presence of compression wood for example (Alméras et al., 2005; Gryc and Horáček, 2007). The second was the challenge of matching two types of measurements: RW from high-resolution RGB images (regardless of the method of measuring RW, manual in our case) and wood density from a fast but lower resolution X-ray scan of the whole disc. The second objective was to test the relevance of this new method by analysing the data collected. For this purpose, a model describing RD as a function of RW, cambial age and height in the tree was proposed and compared to other models in the literature. In order to demonstrate the relevance of our method, we formulated the following hypotheses, based on

the literature review:

- **H1**: Juvenile and mature wood can be delimited by analysis of radial density variations; with mature wood corresponding to the zone where density variations become less important;
- **H2**: There is a negative correlation between RW and RD in Norway spruce, at least in the mature wood;
- **H3**: The RW–RD relationship is valid whatever the height in the tree. This relationship has been relatively little studied at heights in the tree other than breast height.

2. Materials and Methods

2.1. Sampling

Logs were sampled from a Norway spruce plantation near Corcieux (48.1968 N; 6.8869 E, Grand-Est region, France). The trees were about 55 years old. Unfortunately, the history of silvicultural interventions in this stand was not available. A clear cut was carried out on the site in March 2019. The logs were already cut at the time of sampling. One hundred logs with a length of 4.5m were selected for our study. In our sampling, it was therefore possible that several logs belonged to the same tree but the information was not available. One 5cm thick disc was sampled at each end of the log ($n = 200$ discs in total). The discs were labelled with the log number (from #1 to #100) and the position of the disc in the log (bottom or top). The positions were recorded as "gb" for discs sampled at the bottom of the logs and "fb"

for discs sampled at the top of the logs. For example, "E001.fb" was the disc sampled at the top of log number #1.

2.2. Preliminary data processing

The position of each log in a given tree was unknown. However, as all trees were of the same age, the number of growth rings in the discs gave information on the height of the disc, even though each tree has not had exactly the same growth in height. A histogram of the distribution of the number of rings on the 200 discs (Fig. 1) was made to assign each disc and log a level of height in the stem. Looking at the distribution of the number of rings on the discs taken from the bottom of the logs (blue bars in Fig. 1), three modes are clearly visible, suggesting that there were three height levels for the logs. Three positions $p = 1$, 2 or 3 were assigned to the logs according to the number n of rings at their lower end, such that $n > 47$, $47 \geq n > 39$ and $n \leq 39$, respectively. Disc height levels were deduced from the log positions: The bottom disc of a log at position p was set at p while the top disc was set at $p + 1$. The heights in the stem at approximately 0m, 4.5m, 9m and 13.5m were then assigned for each position 1, 2, 3 and 4, respectively.

The numbers of bottom discs obtained at positions 1, 2 and 3 were 46, 43 and 11, respectively. Consequently, the numbers of top discs obtained at positions 2, 3 and 4 were also 46, 43 and 11, respectively. All the discs collected were measured as described in Sections 2.3 and 2.4 but, in order not to oversample height levels 2 and 3, only the 100 bottom discs plus the 11 top discs at position 4 were used in the analyses presented below.

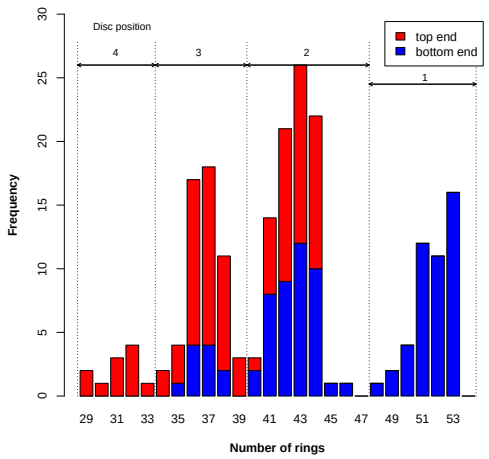

Figure 1: Histogram of the number of rings for the 200 discs (bottom discs in blue and top discs in red). Three height positions $p = 1$, 2 or 3 were assigned to the logs according to the number n of rings in their bottom disc such that $n > 47$, $47 \geq n > 39$ and $n \leq 39$, respectively. The bottom disc of a log at position p was set at p while the top disc was set at $p + 1$.

2.3. Wood density measurements

After air-drying for several months in a ventilated room, the discs were scanned with a General Electric Brightspeed Excel medical X-ray scanner. X-ray computer tomography (CT) allows a 3D reconstruction of an object according to the absorption of X-rays by the object. The scanner settings were: 80 kVp, 50 mA, “DETAIL"" convolution filter and a slice thickness of 1.25mm. Cross-sectional images of the discs were obtained with a resolution of 0.5 to 1 pixels/mm depending on the diameter of the discs.

The grey levels of the raw images are expressed in a standardised unit called the Hounsfield Unit (HU), which allows comparison between images from different scanners. Calibration is done so as to obtain a value of 0

HU in water and -1000 HU in air. In addition, the wood-specific calibration protocol described by Freyburger et al. (2009), based on the analysis of HU measured on various wood species, was applied. After calibration, each pixel in the CT-image is assigned a value corresponding to the density of the wood at that point.

In practice, about ten discs were positioned vertically and scanned in a single pass, resulting in a stack of CT-images. Then, a single CT-image corresponding to each disc was isolated from the image stack.

The 200 CT-images were then processed with ImageJ software (Schneider et al., 2012). The under-bark boundary of the disc and the position of the pith were first recorded using a plug-in called "Gourmand" (Colin et al., 2010).

The manually annotated images were then processed by a second plug-in called "Sectoriseur" (Longuetaud et al., 2016). The "Sectoriseur" plug-in creates, for each disc image, artificial rings of configurable average width (Fig. 2) centred on the pith. This width was set to 1 mm, considering the resolution of the CT images (0.5 to 1 mm per pixel). The plug-in takes as input the average radius of the disc and the desired average width of the artificial rings to calculate how many artificial rings are needed, and then divides each radius ($n = 360$ radii) by this value. Each artificial ring is then assigned an air-dried density value equal to the average density of the pixels within it (background pixels with a density of less than 100 $kg.m^{-3}$ are not considered). These artificial rings are derived from the outer boundary of the wood disc and do not necessarily follow the actual annual growth rings. Artificial rings may intersect actual rings or encompass several rings at the

same time. The expected accuracy for wood density is therefore not at the ring level but rather at the ring group level. The artificial rings may not follow the actual rings at all in the case of irregularly shaped wood discs or where knots are present within the discs (e.g., Fig. 2 on the right). In the case of very regular shaped discs (circular or oval) the accuracy is better.

All density measurements (one row per artificial ring) were saved in the `density` dataset.

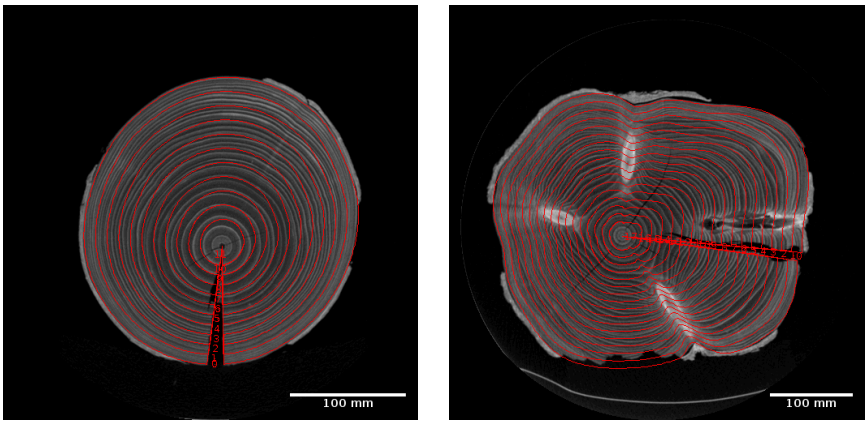

Figure 2: Artificial rings obtained with the "Sectoriseur" plugin (Longuetaud et al., 2016). To facilitate visualisation, the average width of each ring was set at 10mm instead of 1mm.

2.4. Ring width measurements

The measurements of *RW* were made using WinDENDRO software (WinDendro, 2021) on four orthogonal radii for each wood disc. The resolution used was set at 400dpi. A binocular magnifying glass was used to check the first rings near the pith when the ring boundaries were difficult to see with the naked eye.

Then, for each growth ring, an average width was obtained by subtracting the root mean square of successive external and internal radii (each calculated from the values measured on the four radii). This average RW was used in this study.

A calendar year of growth (GY) and a cambial age (CA), *i.e.*, the ring number counted from the pith, were associated with each annual ring.

All RW measurements (one row per annual ring) were recorded in the `ringwidth` dataset.

2.5. Coupling of ring width and density measurements

The objective was to obtain a density value for each individual ring of a disc (RD). For this purpose, the `ringwidth` dataset containing the RW measurements of each annual ring and the `density` dataset containing the density values of each artificial ring of 1mm width (on average) were used.

A scale normalisation, using relative radial positions from 0 to 1, was used to link the two datasets. The coupling algorithm (Fig. 4) first consisted of establishing, from the dataset `density`, an approximation function f of wood density at any relative radial position by linear interpolation from the artificial ring density data. The function `approxfun` of R generates a function that performs such interpolation. Thus, from a given set of x_i values (the relative radial positions of the artificial rings) and corresponding y_i values (the air-dried density of the artificial rings), the generated function f returns for any relative radial position x_j a linearly interpolated density value $y_j = f(x_j)$. Then, for each actual ring of a disc, 100 relative radial positions x_j were considered to generate 100 density values y_j. The average density of a given annual ring was obtained as the average of the corresponding 100 y_j

values. An example of the output of the algorithm is given in Fig. 3.

The two types of measurements did not always match perfectly, as shown by the offset, for the widest rings, between the density maxima (which should be at the outer end of the rings) and the actual ring boundaries (Fig. 3). However, at the scale of a whole ring or a few rings, the overall variations in RD and RW seemed quite consistent.

At the end of this step, each annual ring of a disc could be described by its CA, GY, RW and RD values.

2.6. Annual ring density models from the literature

Several RD prediction models that had been developed for spruce (Table 1) were tested and fitted to our dataset. We mainly present models that take as input explanatory variables available in our dataset (i.e., cambial age, RW and estimated height in the stem). Bouriaud et al. (2015) proposed several models with RW and either cambial age or diameter of the stem at 1.30 m as explanatory variables. As the diameter at 1.30 m was not available in our dataset, only the models with cambial age could be tested. Piispanen et al. (2014) compared the ring density of Norway spruce for even-aged and uneven-aged stands and fitted a model accordingly. In their study, Molteberg and Høibø (2007) proposed more efficient but more complex models taking as input the site fertility index, diameter at 1.30 m and tree height but we do not present them in Table 1 as we have none of these variables on our trees. Even earlier, Olesen (1977) proposed a model depending only on RW for comparison between several cambial ages demonstrating the importance of the two variables, RW and cambial age.

Table 1: Equations found in the literature for predicting tree ring density (RD) for spruce. Only equations taking as inputs RW, cambial age and/or height in the tree were retained.

References	Number of trees	Equations
Bouriaud et al. (2015)	12	(1) $RD_{ij} = a_0 + a_1 RW_{ij} + a_2 RW_{ij}^2 + \frac{a_3}{X_{ij}^{0.5}}$ (2) $RD_{ij} = a_0 + \frac{a_1}{1+RW_{ij}} + \frac{a_2}{X_{ij}^{0.5}}$ (3) $RD_{ij} = a_0 + a_1 RWij^{a_2} + \frac{a_3}{X_{ij}^{a_4}}$ with i the tree, j the year, RD the ring density (air dry), RW ring width and X either the cambial age or the diameter at 1.30 m
Piispanen et al. (2014)	123	$RD_{ij} = a_0 + a_1 CA_{ij} + a_2 CA_{ij}^2 + a_3 \ln(CA_{ij}) + a_4 \ln(RW_{ij})$ $+a_5 \ln(RW_{ij}) CA_{ij} + a_6 DBH_i / Ddom$ with i the tree, j the year, RD the ring density (air dry), RW the ring width, CA the cambial age, DBH the diameter at 1.30m and $Ddom$ the mean diameter of the 100 thickest trees per hectare
Molteberg and Høibø (2007)	46	(1) $RD_{ij} = a_0 + a_1 CA_{ij}$ (2) $RD_{ijk} = a_0 + a_1 H_{ik} + a_2 \ln(H_{ik} + 1) + a_3 CA_{ijk}$ with i the tree, j the year, k the disc, RD the basic density of the sample, H the height of the measurement, CA mean of the cambial age of the sample
Grammel (1990) in Lindström (1996b)	unknown	$RD_{ij} = a \exp(bRW_{ij})$ with i the tree, j the year, RD the ring basic density and RW the ring width
Olesen (1977)	≈ 150	$RD_{ij} = a_0 + \frac{a_1}{RW_{ij}+a_2}$ with i the tree, j the year, RD the ring basic density and RW the ring width
Hakkila (1968) in Lindström (1996b)	unknown	$RD_{ij} = a + b \log(RW_{ij})$ with i the tree, j the year, RD the ring basic density and RW the ring width

2.7. Statistical analysis

Data processing was carried out with the R software (R Core Team, 2021). Regressions were fitted to describe the variations of RD as a function of explanatory variables available in our study: RW, CA and the height level in the stem (H). The main functions used were: `t.test`, `lm`, `nls`, `anova`, `AIC` from **stats** package, `nlsLM` from **minpack.lm** package, and `nlsList`, `nlme` from **nlme** package.

For modelling purposes, we chose to retain most of the annual rings belonging *a priori* to juvenile wood but to remove the very first ring (ring number #1) from each disc, which was clearly much lower in density than subsequent rings. This strong increase would have been difficult to model as

it only occurs between rings one and two, and was of limited interest given the small area represented by these rings as also highlighted by Molteberg and Høibø (2007).

3. Results

3.1. Descriptive analysis

Depending on the height in the stem, the averaged air-dry densities RD plotted against RW followed more or less the same trend: a decrease of RD when RW increases (Appendix A). The rings at the bottom of the stems were denser than those at other height levels for RW greater than approximately 3mm.

As proposed by Saranpää (1994), the juvenile wood limit was set at 10 rings in order to analyse the potential effect of juvenile wood on the RW–RD relationship (Fig. 5 and Table 2). In rings considered mature by this definition, a significant negative RW–RD correlation was observed at each height level. In juvenile wood, the relationship between RW and RD was only observed at stem bottom (0m) and shifted upward compared to mature wood. Juvenile wood was significantly less dense, on average, than mature wood, except at the base of the tree where it was significantly denser (confirmed by a Student t-test for each height level given in Appendix B).

Plots of RD and RW as a function of cambial age (Fig. 6) and growth year (Appendix C) help refine these observations. Regardless of height level, a density peak is observed at ring #2, followed by a decrease in density until approximately ring #10, and finally an increase for the higher cambial ages toward the bark. The density minimum, around ring #10, seems to occur

Table 2: Slope parameters and significances for the eight regressions between air-dry density (RD) and ring width (RW) presented in Fig. 5. Rings less than 10 years old were assumed to belong to juvenile wood. The statistical significance is indicated by: ns: $p \geq 0.05$; *: $0.05 > p \geq 0.01$; **: $0.01 > p \geq 0.001$; ***: $p < 0.001$.

Height in the stem (m)		0	4.5	9	13.5
Juvenile wood	Slope	-22.15	0.39	0.24	-7.89
	P-value	$***$	ns	ns	$*$
Mature wood	Slope	-18.14	-35.12	-30.01	-16.35
	P-value	$***$	$***$	$***$	$***$

closer to the pith as the height level increases in the tree (i.e., for cambial age >10 at the base of the tree and <10 higher up).

By observing the annual variations of the correlation coefficient with CA (Fig. 7), it appears that the level of correlation is stable except around the density minimum near ring #10 where the correlation coefficient becomes close to zero.

The analysis of RW variations according to calendar year (Appendix C) allows us to make some assumptions about the history of the stand: It suggests for instance a thinning around 1992 (followed by an increase in RW), a drought event in 2003 (decrease in RW), as mentioned by Martinez-Meier et al. (2008), and probably another thinning around 2006.

Logically, the density curve appears smoother because the density measurements were averaged over the artificial rings which do not exactly follow the actual rings. However, it was interesting to observe a general decrease in density and ring width in subsequent years.

Fig. D.1 in Appendix D, which can be compared to the similar plot of Wimmer and Downes (2003), does not show a clear effect of growth year on the RW–RD relationship except for the last years (starting around 2017) where the correlation coefficient begins to increase toward zero.

3.2. Statistical analysis

On the basis of the previous observations, statistical models were fitted to describe the variations of RD as a function of RW, CA and H.

A piecewise linear regression of RD with a first breakpoint at cambial age $CA = x_0$ (in juvenile wood) and a second breakpoint at growth year $GY = y_1$ (for the limit before the last decline of both RD and RW toward bark) was first fitted on the whole dataset (except ring at $CA = 1$; see Section 2.7). Full details of this preliminary modelling, including equations and parameter estimates, are given in Appendix F. Most parameters were found to vary as an exponential function of disc height, but the parameter y_1 was found to be constant and equal to 2009.5 regardless of disc height, showing that the decline in RD and RW began in 2009. The latter decline was therefore probably related to an external event (presumably an attack by the European spruce bark beetle *Ips typographus*) and not to a classical evolution related to tree ontogeny.

For this reason, we decided to focus on modelling the first two parts as a function of CA, RW and H (i.e., primarily ontogeny-related variation). After removing the first ring ($CA = 1$) and the last growth years ($GY > 2009$), the final dataset included 3846 rings. The following model (Eq. 1) was first used:

$$RD = \begin{cases} a \cdot CA + b, & \text{if } CA \leq x_0 \\ c \cdot \exp(d \cdot CA) + e, & \text{if } CA > x_0 \end{cases} \quad (1)$$

where $e = a \cdot x_0 + b - c \cdot \exp(d \cdot x_0)$.

Then, mixed models including a random effect corresponding to the height level on the different parameters (tested one after the other) showed that the parameters x_0, b and c varied with the height in the tree, especially at the bottom of the tree (see details in Appendix G). The following equations (Eq. 2) were therefore used to account for this:

$$\begin{aligned} x_0 &= x_{01} \cdot \exp(H)^{-1} + x_{02} \\ b &= b_1 \cdot \exp(H)^{-1} + b_2 \\ c &= c_1 \cdot \exp(H)^{-0.5} + c_2 \end{aligned} \quad (2)$$

The parameters of the final model #1 were thus: a, b_1, b_2, c_1, c_2, d, x_{01} and x_{02} and their estimates and standard errors are given in Table 3. The RMSE, relative RMSE and AIC are given in Table 4. In Fig. 8 the model was used to simulate air-dry density for several height levels and to plot the results as a function of cambial age and calendar year. It appeared that the relationship between RD and CA was very different at the base of the tree compared to the other height levels (on the left). For a given CA, RD tended to be higher at 0m than at other height levels in juvenile wood and lower in mature wood. More generally, for a given CA and in mature wood, RD tended to increase with increasing height in the stem. For a given calendar year and in mature wood, the RD tended to decrease with increasing height

311 in the tree (ignoring the 0m height). The model predictions and observations
312 are shown in Fig. 9.

313 The analysis of the residuals as a function of RW showing a clear trend
314 (Fig. G.2 in Appendix G), the effect of RW was introduced in the following
315 way:

$$
\begin{aligned}
X_{RW} &= f \cdot \exp(RW)^{-1} + g \cdot RW \\
RD &= \begin{cases} a \cdot CA + b + X_{RW}, & \text{if } CA \leq x_0 \\ c \cdot CA + e + X_{RW}, & \text{if } CA > x_0 \end{cases}
\end{aligned} \tag{3}
$$

316 where $e = (a - c) \cdot x_0 + b$.

317 The parameters x_0, b and c depended on the height in the stem following
318 the same equations as for model #1 (Eq. 2).

319 The parameters of the final model #2 were thus: a, b_1, b_2, c_1, c_2, x_{01}, x_{02},
320 f and g and their estimates and standard errors are given in Table 3. The
321 RMSE, relative RMSE and AIC are given in Table 4. This model including
322 RW was only slightly better than the one including only CA and H. The
323 model predictions and observations are shown in Fig. 9.

Table 3: Parameters obtained when fitting the models (estimates and standard errors in brackets): Model #1 taking as input cambial age (CA) and height in the tree (H) (Eq. 1 and 2) and model #2 taking as input CA, H and RW (Eq. 2 and 3).

	a	b_1	b_2	c_1	c_2	d	x_{01}	x_{02}	f	g
Model #1	-2.22e+01	1.21e+02	4.93e+02	1.62e+02	-4.08e+02	-2.81e-02	4.23e+00	6.12e+00		
	(7.71e-01)	(3.70e+00)	(3.97e+00)	(2.74e+01)	(3.82e+01)	(5.17e-03)	(1.84e-01)	(1.43e-01)		
Model #2	-1.49e+01	8.88e+01	5.16e+02	-3.16e+00	5.30e+00		4.27e+00	7.33e+00	6.79e+01	-7.83e+00
	(6.43e-01)	(3.36e+00)	(4.84e+00)	(2.10e-01)	(1.73e-01)		(2.51e-01)	(2.02e-01)	(8.24e+00)	(6.37e-01)

Table 4: Comparison of our models (#1 and #2) with other models from the literature for Norway spruce. The models have been here fitted on annual rings from years ≤ 2009 and excluding the ring number one of each disc.

References	Equation number	Df	RMSE (kg.m^{-3})	Relative RMSE (%)	AIC
Bouriaud et al. (2015)	(1) in Table 1	3842	51.73	11.50	41277
	(2) in Table 1	3843	52.48	11.66	41386
	(3) in Table 1	3841	51.28	11.40	41212
Piispanen et al. (2014)	-	3840	48.58	10.80	40799
Molteberg and Høibø (2007)	(2) in Table 1	3842	59.84	13.30	42398
Grammel (1990) in Lindström (1996b)	-	3844	54.37	12.08	41657
Olesen (1977)	-	3843	52.65	11.70	41412
Hakkila (1968) in Lindström (1996b)	-	3844	52.79	11.73	41429
Model #1 taking as input CA and H	(1) and (2) in Section 3.2	3838	44.98	9.99	40209
Model #2 taking as input CA, H and RW	(2) and (3) in Section 3.2	3837	42.40	9.42	39758

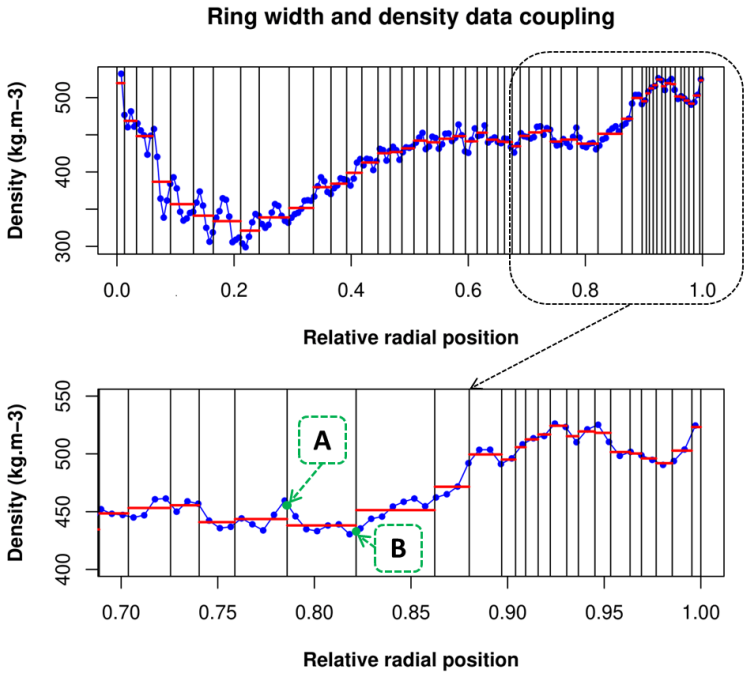

Figure 3: Coupling of ring width and density data over the whole radius of the disc (top) and zooming in on a part of the radius (bottom). The blue points represent the air-dry densities of the artificial rings obtained every millimetre. The black vertical lines are the boundaries of the actual annual rings. For a given actual ring, a sequence of 100 radial positions was considered. A and B are the points of intersection of the density curve of the artificial rings (in blue) with the boundaries of the actual ring considered. For each of the 100 radial positions (i.e., between points A and B), a density value was generated by means of an interpolation function. Finally, for a given actual ring, the horizontal red segment represents the average density obtained from the 100 interpolated density values. The case of the disc "E001.gb" is presented.

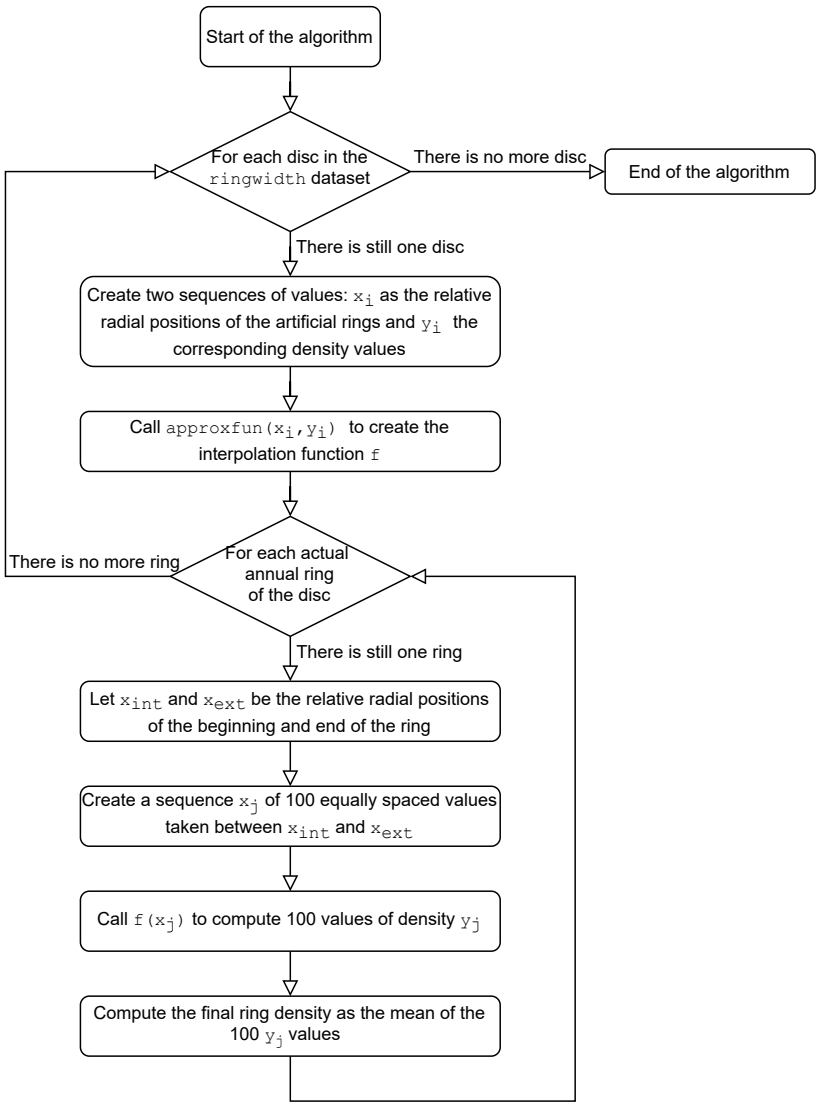

Figure 4: Diagram of the coupling algorithm.

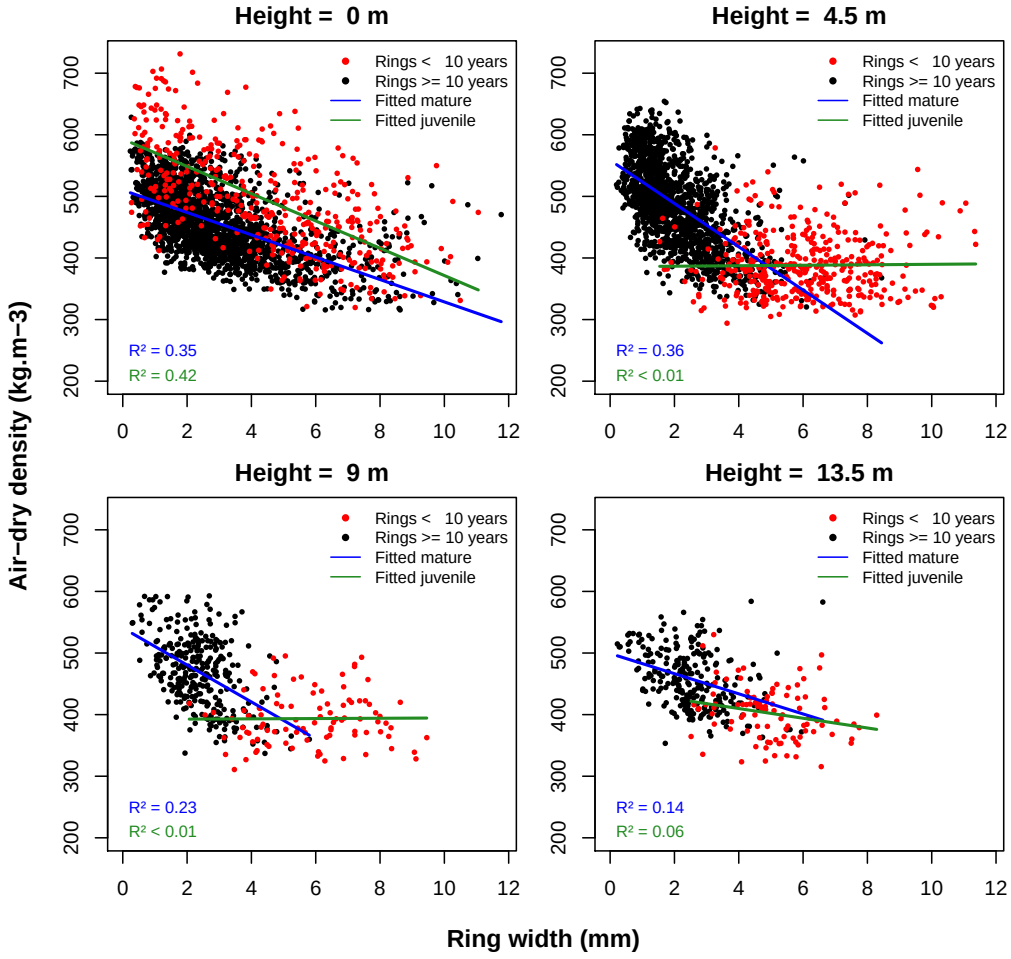

Figure 5: Air-dry density versus ring width (RW) for the different heights in the stem (0m, 4.5m, 9m and 13.5m) distinguishing juvenile wood (red points) from mature wood (black points). Regression lines were fitted for juvenile wood (in green) and for mature wood (in blue).

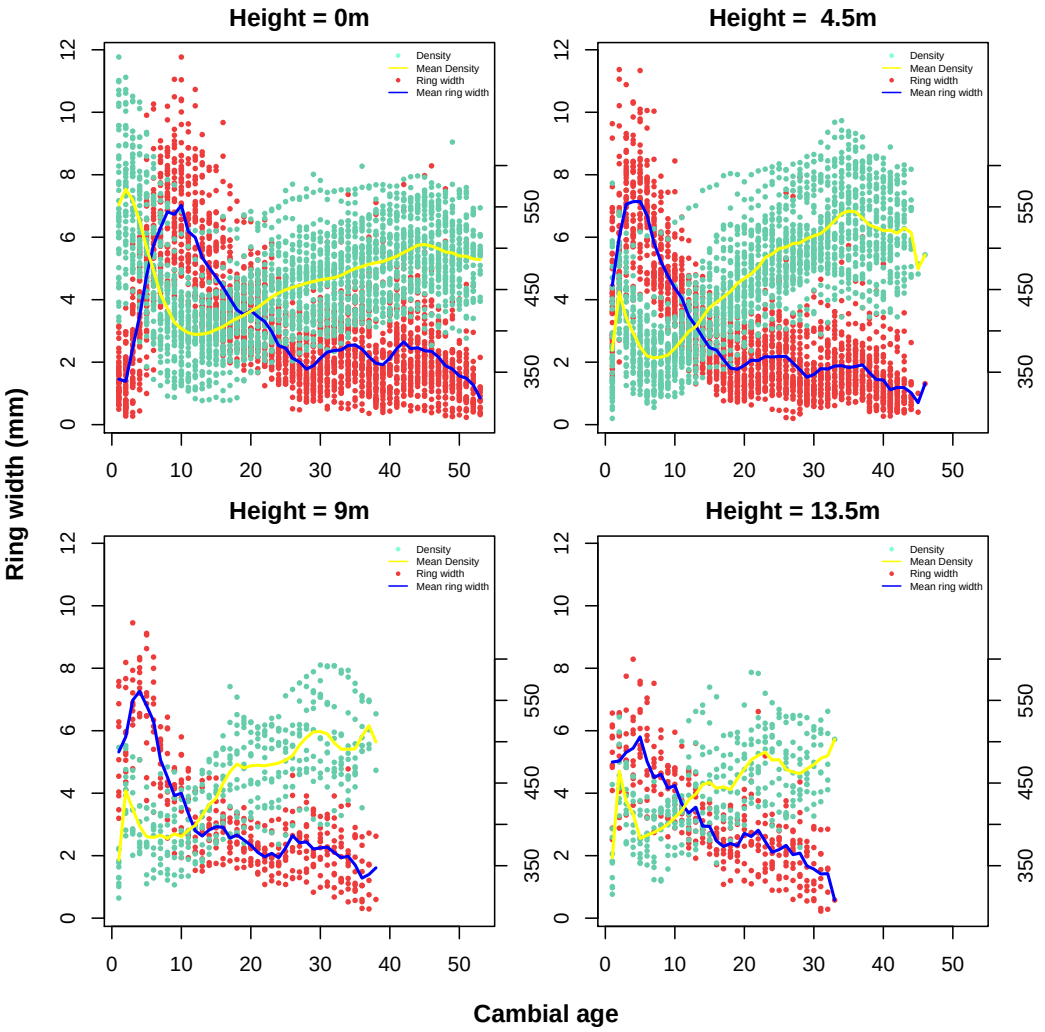

Figure 6: Ring width (red points) and air-dry density (green points) as a function of cambial age for the different heights in the stem (0m, 4.5m, 9m and 13.5m). Trend curves for ring width (in blue) and density (in yellow) are plotted.

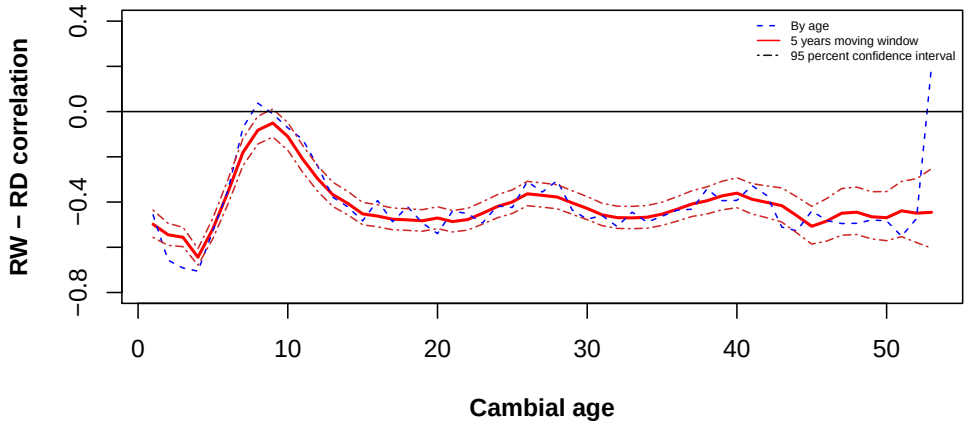

Figure 7: Pearson correlation coefficient between air-dry ring density (RD) and ring width (RW) as a function of cambial age, including all height levels. The coefficients are computed for each cambial age (dashed blue line) and then using a five years moving window for the computation to obtain a smoothed curve (red line). A 95% confidence band is plotted for the smoothed curve (dashed red line).

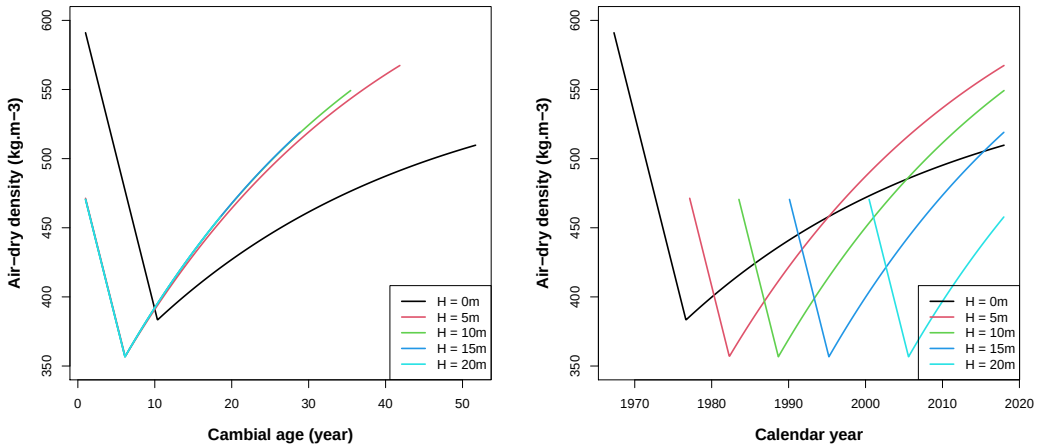

Figure 8: Simulations of air-dry density obtained by using model #1 for several height levels (0m, 5m, 10m, 15m and 20m). The model was used in extrapolation for heights 15m and 20m. The average total number of rings at each height level was extrapolated with the `splinefun` function of R (Appendix E).

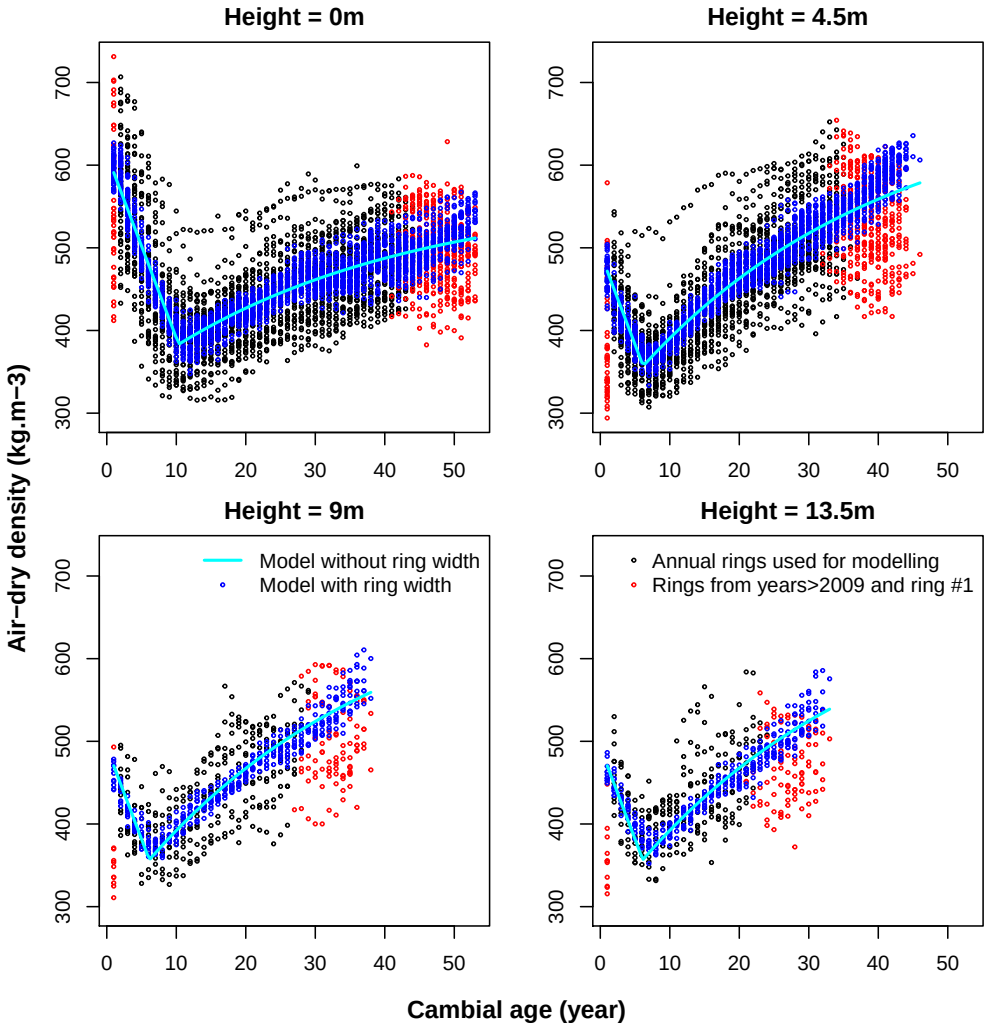

Figure 9: Observations and model predictions for each height level. Black dots correspond to data that were used for fitting the models. Red dots correspond to data that were not used for fitting the models (i.e., rings number one and rings from years $>$ 2009). Predictions from the model that does not include ring width (RW) are in cyan (model #1; Eq. 1 and 2) and predictions from the model that includes RW (model #2; Eq. 2 and 3) are the blue dots.

4. Discussion

4.1. Factors involved in ring density variations

4.1.1. Cambial age

The radial patterns of *RD* that were observed in our study are consistent with the most common results found in the literature (e.g., Olesen, 1977; Petty et al., 1990; Molteberg and Høibø, 2006). Olesen (1977) reported a density higher than that of mature wood for the innermost rings (density is maximum at ring #3), then a decrease in density until rings #8-10 and then an increase until reaching the average density of mature wood around rings #15-20. Saranpää (1994) also chose to focus on the first 10 rings to study the juvenile wood. In these 10 rings, the author observed a maximum of density at ring #2 or #3 and then a decrease. In young Norway spruce trees, Molteberg and Høibø (2006) found the minimum of density around rings #5-8 followed by an increase in density towards the bark in mature wood. This is the most commonly reported pattern for radial variations in density, although differences are sometimes observed depending on stand type (e.g., Petty et al., 1990; Piispanen et al., 2014), social status of the trees or site fertility (e.g., Molteberg and Høibø, 2007), or fertilization (Lindström, 1996b). Piispanen et al. (2014) observed that trees in uneven-aged stands had a very high density in the juvenile wood near the pith, then density decreased until about ring #20 before rising again and decreasing slightly at the end near the bark, which is a fairly typical pattern except for the final decrease towards the bark. The density peak near the pith as well as the decrease in density for the outermost rings were not observed for even-aged stands. In our case, in an even-aged stand, the maximum density was

observed at ring #2, then a decrease in density was observed until ring #10 and finally the RD increased continuously from ring #10 to around ring #45. At the bottom of the stem, the average density of the 10 first rings was higher than the average density of mature wood. For the other height levels, the overall patterns were about the same, but with a lower density in the innermost rings and in juvenile wood in general. Such results suggest that the limit between juvenile and mature wood was around ring #10. However, this limit appeared to depend on the height in the stem for our sample. On the basis of our model #1, the limit was estimated at ring #10 at 0m, #7 at 1.30m and #6 at 15m. These results, which support Hypothesis **H1**, but with a variation according to the height in the tree, are original and have not been found in the literature.

According to Olesen (1977), the strong decrease in density in juvenile wood is related to a rapid increase in tracheid width in these first rings (as an example, there are five times as many tracheids per unit area in the innermost rings as in mature wood) although the cell walls are relatively thin, particularly in the late wood. For Jyske et al. (2008), the decrease in density in juvenile wood is due to a decrease in early wood density, which is not inconsistent with the observation made by Olesen (1977). At the same time, the proportion of late wood as well as its density increases with cambial age (Olesen, 1977; Jyske et al., 2008) and this explains the increase in density from juvenile wood outward.

This is broadly consistent with the observation that wood formed around the pith in softwoods is of lower density than wood formed outside (Lachenbruch et al., 2011).

The presence of compression wood of higher density than normal wood in the first rings near the pith may also help explain the trend of decreasing wood density observed in juvenile wood (Gryc and Horáček, 2007).

4.1.2. Ring width

In our study, the negative *RW*–*RD* relationship was observed regardless of height in the stem in mature wood, thus supporting the Hypothesis **H2**. A negative correlation between *RW* and *RD* has often been reported for Norway spruce (e.g., Lindström, 1996a; Bouriaud et al., 2015).

At stem bottom, as reported by Olesen (1977), the slope of the negative *RW*–*RD* relationship was almost the same for juvenile and mature wood but, for the same *RW*, the density was often higher in the juvenile wood. In our study, a quite constant negative correlation was found in mature wood, much more constant than what was observed in the study of Wimmer and Downes (2003). In juvenile wood at other height levels, there was little or no relationship between *RD* and *RW*, invalidating hypothesis **H3**. The observed increase of *RW* from about 1 to 7mm on average during the first 10 years at stem bottom could allow the young tree to delay material allocation until leaves and roots are sufficiently developed, while the decrease in density would correspond to an increased need for hydraulic conductivity. Later in the tree life, the decrease in *RW* (and especially of early wood width, leading to an increase in late wood proportion and thus in *RD*) could make the conductive area of the rings to remain broadly constant. From a biomechanical point of view, there is also an interest for the young tree to be flexible so as not to break under the effect of the wind, whereas a larger tree must gain in rigidity by building denser wood so as not to fall. The tree must invest in its

structural stability as it grows. According to Lindström (1996a), crown development acts as a primary regulator of wood structure and density through four independent theories of wood formation (mechanical theory, nutritional theory, water conduction theory and hormonal theory). The author points out that the size of the crown influences the transpiration requirements and therefore the proportions of conduction tissue and strength tissue (early- and latewood).

4.1.3. Height in the stem

As shown by the relationships between the model parameters and H (Appendix G.1), the changes in density with height in the stem were more pronounced at the stem base. From our model, it thus appeared that the RW–RD relationship varied with height in the stem, contradicting Hypothesis **H3** of stability of the relationship. In the absence of measurements between 0 and 4m height in our study, precise variations in density could not be assessed, but it is likely that the effect of height is not negligible at breast height, at which density data are most often measured. Although according to several studies cited by Saranpää (1994), species in the genus *Picea* show only slight changes in wood properties with height.

As can be seen from our results, juvenile wood tended to be denser on average at the base of the tree. While for the other height levels, the density was on average lower in juvenile wood than in mature wood.

In juvenile wood, RD at stem base was found to be higher than RD at the same cambial ages at 4.5 m or higher in the stem (see model simulations). Conversely, the density of mature wood for given cambial ages tended to increase with height in the tree, but the important difference in RD was

primarily observed in our study between the base of the tree and the rest of the stem. The increase in density with height in the stem for given cambial age classes was also observed by Molteberg and Høibø (2006) and Jyske et al. (2008), and would be related to apical meristem maturity (Jyske et al., 2008).

Inversely, model simulations showed that for a given GY, RD tended to decrease with increasing height in the tree, in agreement with the results of Olesen (1977) and Jyske et al. (2008). This decrease in density can logically be explained by the increase in RW with height in the tree for a given calendar year, associated with the decrease in latewood proportion, and also with the increase in the proportion of juvenile wood (Jyske et al., 2008). Olesen (1977) explained this decrease in density by a greater width of tracheids toward the top of the tree in a given ring.

On a more global scale, Gryc and Horáček (2007) observed on one *Picea abies* tree a decrease in density with increasing height in the stem in a region of the stem including compression wood, while density was slightly increasing in the region of opposite wood. Molteberg and Høibø (2007), at the disc level, observed a decrease in density from butt end to 7-8 m.

4.2. Statistical modelling

Several models from the literature, as shown in Table 4, were fitted to our data, and new models were developed, that were more suitable for describing both the radial and vertical variations of RD. It should be noted that the purpose of developing new models was primarily to be able to explain our data. They are therefore explanatory models rather than predictive models. The results obtained are relevant compared to others found in the literature and prove that our new method is relevant to obtain fully exploitable data

of high scientific value. In particular, an important difference, not often mentioned in the literature, was highlighted between juvenile wood at the base of the tree (of higher density) and juvenile wood at other height levels.

4.3. Juvenile wood definition

Analysis of the *RW–RD* relationship and the observed variations in juvenile wood raise questions about the definition of juvenile wood area and its variation with height in the stem. For Saranpää (1994), the properties of juvenile wood change with height in the stem. Lachenbruch et al. (2011), quoting Larson (1969), pointed out that the term juvenile wood is more appropriate for wood formed by young trees, *i.e.*, at the base of the tree, while corewood (or also sometimes crown-formed wood) is more appropriate for wood formed near the pith but higher up. Finally, Burdon et al. (2004) proposed a new terminology where juvenility *versus* maturity is appropriate for vertical variations while corewood *versus* outerwood is rather for radial variations. Through our study we have indeed highlighted important differences between juvenile wood formed at the base of the tree and that formed higher up, and it appeared important to distinguish these two types of wood. It would also be interesting to make other measurements to study the correspondence between the patterns of radial density variation and those of fibre length or microfibril angle, for example.

4.4. Methodological aspects

We found in our data the classical pattern of radial density variation for Norway spruce: First a decrease in density from a ring near the pith to a minimum around ring #10 and then an increase towards the bark (Jyske

et al., 2008). The original coupling method developed for this study therefore seems appropriate to obtain relevant data in agreement with the main results of the literature.

A likely source of uncertainty was that density was measured on the whole discs while ring width was measured on four orthogonal radii whose location on the discs was not precisely known. For a better match, it might be more efficient in the future to cut four radial strips to ensure that the same regions of the discs are measured for density and ring width.

This method allowed us to go even further with original results on the vertical variations of the radial density variation pattern and the RW–RD relationship, relatively unstudied in the literature, and also on particular phenomena such as the drop in density from the year 2009. We do not know what is responsible for this sudden decrease but one hypothesis would be an attack by the European spruce bark beetle *Ips typographus*. The phenomenon of fungal infestation associated with an attack of the bark was proved to reduce drastically the wood quality with also weight losses (Hỳsek et al., 2021). The degree of degradation depends on the duration of the fungi activity. Before three years, there is no strong loss of quality. In our study, the decrease in wood density was observed for the last 10 years of growth.

5. Conclusion

The proposed method is suitable to process wood discs and does not require extensive sample preparation or long X-ray image acquisition time. It has the advantage of measuring the density over the entire surface of the discs. The method is original because it makes it possible to couple precise

497 RW measurements made on high-resolution colour images with high-speed
498 density measurements made on lower resolution X-ray images, without any
499 sample preparation. The initial idea of this work was to propose an inter-
500 mediate method, a little less accurate but faster than the classical methods
501 used in dendrochronology, which require fine and time-consuming sample
502 preparation.

503 The primary objective of this work was to provide data for research on
504 density variation in the tree (radially and vertically) in relation to volume
505 growth for the purpose of, for example, fitting models. As an example of
506 application, we are currently developing technologies to automatically mea-
507 sure ring widths in industry from RGB images of log cross-sections and these
508 models would be needed to provide information on the quality of these woods.

509 This coupling method proved to be relevant. The coupling between the
510 two types of measurements was conclusive insofar as it made it possible
511 to reproduce the classic trends known through the literature regarding the
512 existing relationships between RW and RD in the case of spruce: Mostly
513 negative relationships. The data obtained allowed us to go further with
514 original and little studied results, notably on the evolution of the radial
515 variation pattern of density and on the RW–RD relationship with height,
516 and to question the definition of the juvenile wood zone.

517 The models fitted on the basis of our data were able to describe the
518 variations of RD with CA, RW and height in the stem.

519 The definition of juvenile wood area and its variations with height in the
520 stem could also be better explored with these data. In our study, density
521 variations in juvenile wood were different at the base of the tree compared

to higher height levels. Juvenile wood at the base of the tree tended to have relatively narrow RW associated with high RD, compared to juvenile wood formed at higher height levels and even to mature wood formed at the base of the tree. A negative RW–RD relationship was observed in juvenile wood at the base of the tree but not at other height levels. This study therefore validates the relevance of distinguishing between juvenile wood formed at the base of the tree and that formed higher up as several authors have also suggested.

The simulations of air-dried RD using the developed models allowed to conclude that for these spruce trees the variations in RD were more influenced by CA than by the height in the tree except at the base of the tree where the trends were really different. The two models developed from our data (one taking into account RW and the other not) showed very comparable results although the model using RW, in addition to CA and height in the stem, was logically better. Compared to other models from the literature, our models were also more accurate, which is only to be expected given that our models were designed for our dataset, but it further validates the relevance of the proposed method. Our models allowed to explore and better understand the variations in wood density of spruce.

The next step would be to apply this method on a larger scale on a better described sample (e.g., through a better knowledge of the stand history, with more measurements at the bottom of the stems) and extended to other species to confirm its interest.

Acknowledgement

Thanks to the forestry cooperative *Forêt et Bois de l'Est* for supplying and delivering the 100 spruce logs to Freiburg. Thanks also to Franka Brüchert of the *Forest Research Institute of Baden-Württemberg* (FVA) and the whole team for their help in organising the measurement and imaging of the logs at FVA. Thanks to Frédéric Bordat, Adrien Contini and Florian Vast for sampling the discs in the field and preparing the samples at INRAE Nancy. Thanks to Adeline Motz and Daniel Rittié for ring width measurements. The authors would like to thank SILVATECH (Silvatech, INRAE, 2018. Structural and functional analysis of tree and wood Facility, doi: 10.15454/1.5572400113627854E12) from UMR 1434 SILVA, 1136 IAM, 1138 BEF and 4370 EA LERMAB from the research center INRAE Grand-Est Nancy, and especially Charline Freyburger for the realisation of the X-ray scans.

References

Alméras, T., Thibaut, A., Gril, J., 2005. Effect of circumferential heterogeneity of wood maturation strain, modulus of elasticity and radial growth on the regulation of stem orientation in trees. Trees 19, 457–467.

Badeau, V., Becker, M., Bert, D., Dupouey, J.L., Lebourgeois, F., Picard, J.F., 1996. Long-term growth trends of trees: ten years of dendrochronological studies in france, in: Growth trends in European forests. Springer, pp. 167–181.

Bontemps, J.D., Gelhaye, P., Nepveu, G., Hervé, J.C., 2013. When tree rings

behave like foam: moderate historical decrease in the mean ring density of common beech paralleling a strong historical growth increase. Annals of forest science 70, 329–343.

Bouriaud, O., Teodosiu, M., Kirdyanov, A., Wirth, C., 2015. Influence of wood density in tree-ring-based annual productivity assessments and its errors in norway spruce. Biogeosciences 12, 6205–6217.

Van den Bulcke, J., Boone, M.A., Dhaene, J., Van Loo, D., Van Hoorebeke, L., Boone, M.N., Wyffels, F., Beeckman, H., Van Acker, J., De Mil, T., 2019. Advanced x-ray ct scanning can boost tree ring research for earth system sciences. Annals of Botany 124, 837–847.

Burdon, R.D., Kibblewhite, R.P., Walker, J.C., Megraw, R.A., Evans, R., Cown, D.J., 2004. Juvenile versus mature wood: a new concept, orthogonal to corewood versus outerwood, with special reference to pinus radiata and p. taeda. Forest science 50, 399–415.

Colin, F., Mothe, F., Freyburger, C., Morisset, J.B., Leban, J.M., Fontaine, F., 2010. Tracking rameal traces in sessile oak trunks with x-ray computer tomography: biological bases, preliminary results and perspectives. Trees 24, 953–967.

De Mil, T., Vannoppen, A., Beeckman, H., Van Acker, J., Van den Bulcke, J., 2016. A field-to-desktop toolchain for x-ray ct densitometry enables tree ring analysis. Annals of botany 117, 1187–1196.

Franceschini, T., Bontemps, J.D., Gelhaye, P., Rittie, D., Herve, J.C., Gegout, J.C., Leban, J.M., 2010. Decreasing trend and fluctuations in

591 the mean ring density of norway spruce through the twentieth century.
592 Annals of forest science 67, 816–816.

593 Franceschini, T., Longuetaud, F., Bontemps, J.D., Bouriaud, O., Caritey,
594 B.D., Leban, J.M., 2013. Effect of ring width, cambial age, and climatic
595 variables on the within-ring wood density profile of norway spruce picea
596 abies (l.) karst. Trees 27, 913–925.

597 Freyburger, C., Longuetaud, F., Mothe, F., Constant, T., Leban, J.M., 2009.
598 Measuring wood density by means of X-ray computer tomography. Annals
599 of Forest Science 66. doi:10.1051/forest/2009071.

600 García-Gonzalo, E., Santos, A.J., Martínez-Torres, J., Pereira, H., Simões,
601 R., García-Nieto, P.J., Anjos, O., 2016. Prediction of five softwood pa-
602 per properties from its density using support vector machine regression
603 techniques. BioResources 11, 1892–1904.

604 Grammel, R., 1990. Relations between growth conditions and wood proper-
605 ties in norway spruce. Forstwissenschaftliches Centralblatt 109, 119–129.

606 Gryc, V., Horáček, P., 2007. Variability in density of spruce (picea abies [l.]
607 karst.) wood with the presence of reaction wood. Journal of forest science
608 53, 129–137.

609 Hakkila, P., 1968. Geographical variation of some properties of pine and
610 spruce pulpwood in finland. Communications Instituti Forestalis Fenniae
611 66, 1–59.

612 Hỳsek, Š., Löwe, R., Turčáni, M., 2021. What happens to wood after a tree
613 is attacked by a bark beetle? Forests 12, 1163.

614 Jacquin, P., Longuetaud, F., Leban, J.M., Mothe, F., 2017. X-ray micro-
615 densitometry of wood: a review of existing principles and devices. Den-
616 drochronologia 42, 42–50.

617 Jacquin, P., Mothe, F., Longuetaud, F., Billard, A., Kerfriden, B., Leban,
618 J.M., 2019. Carden: a software for fast measurement of wood density on
619 increment cores by ct scanning. Computers and Electronics in Agriculture
620 156, 606–617.

621 Jyske, T., Mäkinen, H., Saranpää, P., 2008. Wood density within norway
622 spruce stems. Silva Fennica 42, 439–455.

623 Kerfriden, B., Bontemps, J.D., Leban, J.M., 2021. Variations in temperate
624 forest stem biomass ratio along three environmental gradients are dom-
625 inated by interspecific differences in wood density. Plant Ecology 222,
626 289–303.

627 Kiaei, M., Khademi-Eslam, H., Hooman Hemmasi, A., Samariha, A., 2012.
628 Ring width, physical and mechanical properties of eldar pine (case study
629 on marzanabad site). Cellulose Chemistry and Technology 46, 125.

630 Lachenbruch, B., Moore, J.R., Evans, R., 2011. Radial variation in wood
631 structure and function in woody plants, and hypotheses for its occurrence,
632 in: Size-and age-related changes in tree structure and function. Springer,
633 pp. 121–164.

634 Larson, P.R., 1969. Wood formation and the concept of wood quality. Bul-
635 letin no. 74. New Haven, CT: Yale University, School of Forestry. 54 p. ,
636 1–54.

Lin, C.J., Tsai, M.J., Lee, C.J., Wang, S.Y., Lin, L.D., 2007. Effects of ring characteristics on the compressive strength and dynamic modulus of elasticity of seven softwood species. Holzforschung 61, 414–418.

Lindström, H., 1996a. Basic density in norway spruce. part i. a literature review. Wood and Fiber Science 28, 15–27.

Lindström, H., 1996b. Basic density in norway spruce, part iii. development from pith outwards. Wood and fiber science 28, 391–405.

Longuetaud, F., Mothe, F., Fournier, M., Dlouha, J., Santenoise, P., Deleuze, C., 2016. Within-stem maps of wood density and water content for characterization of species: a case study on three hardwood and two softwood species. Annals of forest science 73, 601–614.

Martinez-Meier, A., Sanchez, L., Pastorino, M., Gallo, L., Rozenberg, P., 2008. What is hot in tree rings? the wood density of surviving douglas-firs to the 2003 drought and heat wave. Forest Ecology and Management 256, 837–843.

Molteberg, D., Høibø, O., 2006. Development and variation of wood density, kraft pulp yield and fibre dimensions in young norway spruce (picea abies). Wood Science and Technology 40, 173–189.

Molteberg, D., Høibø, O., 2007. Modelling of wood density and fibre dimensions in mature Norway spruce. Canadian Journal of Forest Research 37, 1373–1389. doi:10.1139/X06-296.

Olesen, P., 1977. The variation of the basic density level and tracheid width

within the juvenile and mature wood of norway spruce. Forest Tree Improvement (Denmark). no. 12. .

Petty, J., MacMillan, D.C., Steward, C., 1990. Variation of density and growth ring width in stems of sitka and norway spruce. Forestry: An International Journal of Forest Research 63, 39–49.

Piispanen, R., Heinonen, J., Valkonen, S., Mäkinen, H., Lundqvist, S.O., Saranpää, P., 2014. Wood density of norway spruce in uneven-aged stands. Canadian Journal of Forest Research 44, 136–144.

Pretzsch, H., Biber, P., Schütze, G., Kemmerer, J., Uhl, E., 2018. Wood density reduced while wood volume growth accelerated in central european forests since 1870. Forest Ecology and Management 429, 589–616.

R Core Team, 2021. R: A Language and Environment for Statistical Computing. R Foundation for Statistical Computing. Vienna, Austria. URL: https://www.R-project.org/.

Saranpää, P., 1994. Basic density, longitudinal shrinkage and tracheid length of juvenile wood of picea abies (l.) karst. Scandinavian Journal of Forest Research 9, 68–74.

Saranpää, P., 2003. Wood density and growth. Wood quality and its biological basis , 87–117.

Schneider, C.A., Rasband, W.S., Eliceiri, K.W., 2012. Nih image to imagej: 25 years of image analysis. Nature methods 9, 671–675.

Sotelo Montes, C., Weber, J.C., Abasse, T., Silva, D.A., Mayer, S., Sanquetta, C.R., Muñiz, G.I., Garcia, R.A., 2017. Variation in fuelwood properties and correlations of fuelwood properties with wood density and growth in five tree and shrub species in niger. Canadian Journal of Forest Research 47, 817–827.

Steffenrem, A., Kvaalen, H., Dalen, K.S., Høibø, O.A., 2014. A high-throughput x-ray-based method for measurements of relative wood density from unprepared increment cores from picea abies. Scandinavian Journal of Forest Research 29, 506–514.

Todaro, L., Macchioni, N., 2011. Wood properties of young douglas-fir in southern italy: results over a 12-year post-thinning period. European Journal of Forest Research 130, 251–261.

Wimmer, R., Downes, G., 2003. Temporal variation of the ring width-wood density relationship in Norway spruce grown under two levels of anthropogenic disturbance. IAWA journal / International Association of Wood Anatomists 24, 53–61. doi:10.1163/22941932-90000320.

Wimmer, R., Grabner, M., 2000. A comparison of tree-ring features in picea abies as correlated with climate. Iawa Journal 21, 403–416.

WinDendro, 2021. WinDENDRO: An image analysis system for annual tree-rings analysis. URL: https://regentinstruments.com/assets/windendro_about.html.